Can Weakly Coordinating Anions Stabilize Mercury in Its Oxidation State +IV?

Sebastian Riedel,[a] Michal Straka,[a, b] and Martin Kaupp*[a]

Dedicated to Professor Konrad Seppelt on the occasion of his 60th birthday

Abstract: While the thermochemical stability of gas-phase HgF_4 against F_2 elimination was predicted by accurate quantum chemical calculations more than a decade ago, experimental verification of “truly transition-metal” mercury(IV) chemistry is still lacking. This work uses detailed density functional calculations to explore alternative species that might provide access to condensed-phase Hg^{IV} chemistry. The structures and thermochemical stabilities of complexes $Hg^{IV}X_4$ and $Hg^{IV}F_2X_2$ ($X^-=AlF_4^-$, $Al_2F_7^-$, AsF_6^-, SbF_6^-, $As_2F_{11}^-$, $Sb_2F_{11}^-$, $OSeF_5^-$, $OTeF_5^-$) have been assessed and are compared with each other, with smaller gas-phase HgX_4 complexes, and with known related noble gas compounds. Most species eliminate F_2 exothermically, with energies ranging from only about $-60\,kJ\,mol^{-1}$ to appreciable $-180\,kJ\,mol^{-1}$. The lower stability of these species compared to gas-phase HgF_4 is due to relatively high coordination numbers of six in the resulting Hg^{II} complexes that stabilize the elimination products. Complexes with AsF_6 ligands appear more promising than their SbF_6 analogues, due to differential aggregation effects in the Hg^{II} and Hg^{IV} states. HgF_2X_2 complexes with $X^-=OSeF_5^-$ or $OTeF_5^-$ exhibit endothermic fluorine elimination and relatively weak interactions in the Hg^{II} products. However, elimination of the peroxidic $(OEF_5)_2$ coupling products of these ligands provides an alternative exothermic elimination pathway with energies between -120 and $-130\,kJ\,mol^{-1}$. While all of the complexes investigated here thus have one exothermic decomposition channel, there is indirect evidence that the reactions should exhibit nonnegligible activation barriers. A number of possible synthetic pathways towards the most interesting condensed-phase Hg^{IV} target complexes are proposed.

Keywords: anions • density functional calculations • high oxidation states • mercury • reductive elimination

Introduction

Can we turn Group 12 of the periodic table into a true transition-metal group in which the valence d orbitals are involved in bonding? Mainly due to relativistic effects, this becomes most likely for the heaviest group member, mercury[1] (and even more so for eka-mercury, element 112[2]). Indeed, the possible existence of mercury in higher oxidation states than +II has fascinated both experimental and theoretical chemists for years. In 1976 Deming et al.[3] reported the spectroscopic characterization of an electrochemically generated, short-lived $[Hg^{III}(cyclam)]^{3+}$ species, which unfortunately has never been confirmed to date.[4] Based on that report, Jørgensen[5] speculated about the possible existence of Hg^{IV} as HgF_4. In analogy with the experimentally known higher stability of $5d^8$ Au^{III} versus $5d^9$ Au^{II} species, the $5d^8$ Hg^{IV} oxidation state should be more stable than $5d^9$ Hg^{III}.

The first quantum-chemical study of this problem,[1,6] using coupled-cluster methods, predicted square-planar D_{4h} HgF_4 to be thermochemically stable in the gas phase with respect to the principal decomposition pathway $HgF_4 \rightarrow HgF_2+F_2$. It was shown[1] that this stability is mainly due to

---

[a] Dipl.-Chem. S. Riedel, Dr. M. Straka, Prof. Dr. M. Kaupp
Universität Würzburg, Institut für Anorganische Chemie
Am Hubland, 97074 Würzburg (Germany)
Fax: (+49) 931-888-7135
E-mail: kaupp@mail.uni-wuerzburg.de

[b] Dr. M. Straka
Present address: Department of Chemistry
P.O. Box 55 (A.I. Virtasen aukio 1)
University of Helsinki, 00014, Helsinki (Finland)

Supporting information for this article is available on the WWW under http://www.chemeurj.org/ or from the author: Cartesian coordinates of the optimized structures of the major complexes (Table S1), vibrational frequencies (Table S2), and NPA charges of selected complexes (Table S3).

DOI: 10.1002/chem.200401130

relativistic destabilization of the Hg^{II} species[7] (see also reference [8] for the analogous destabilization of Au^{I} halides). Subsequent high-level calculations confirmed the positive reaction energy of F_2 elimination, whereas $HgCl_4$ was found to be thermochemically unstable with respect to Cl_2 elimination.[9,10] The gas-phase hydride species $Hg^{IV}H_4$ and $Hg^{VI}H_6$ were computed to be appreciably endothermic but to have modest barriers for H_2 elimination.[10,11]

In spite of its computed favorable gas-phase thermochemistry, HgF_4 has not yet been confirmed experimentally. Molecular-beam experiments with fluorine and mercury are not attractive to experimentalists, and matrix-isolation spectroscopy has not yet produced evidence for HgF_4 either.[12] In the condensed bulk phase, elimination of F_2 is strongly favored by the much higher aggregation energy of solid HgF_2 in its ionic, high-coordinate fluorite structure compared to aggregation of more covalent square-planar HgF_4.[1] While we consider the matrix-isolation route towards HgF_4 to still be insufficiently investigated, it is appropriate at this point to explore alternative Hg^{IV} targets that might offer easier experimental access.

As the major obstacle to condensed-phase Hg^{IV} chemistry is the energy gain of the corresponding Hg^{II} compounds by aggregation, it seems natural to consider ligands that will not allow high-coordinate Hg^{II} aggregation. One option is to use certain oxidation-stable macrocyclic ligands, on which we will report elsewhere.[13] The other viable option involves weakly coordinating anions, several of which are well known to stabilize high oxidation states as well as unusual and otherwise unstable cations.[14,15] In weakly coordinating anions (WCA), the negative charge is typically delocalized over several centers, and the nucleophilicity of individual connecting ligand atoms is thus low. The idea is that aggregation of Hg^{II} complexes existing in superacid environments that produce WCAs should be considerably less pronounced than that of HgF_2 itself.

Here we explore by quantum-chemical methods the structures and thermochemical stabilities of Hg^{IV} complexes with a variety of WCAs. The aim is to identify appropriate targets for experimental access. We investigate in particular HgX_4 as well as *cis*- and *trans*-HgF_2X_2 complexes, where X^- is one of the following WCAs: AlF_4^-, AsF_6^-, SbF_6^-, the dinuclear anions $Al_2F_7^-$, $As_2F_{11}^-$, $Sb_2F_{11}^-$, and the pentafluorooxotellurate and -selenate anions OEF_5^- (E = Te, Se). For comparison, a number of noble gas compounds are also investigated.

Computational Details

Previous quantum chemical studies on the stability of Hg^{IV} have involved mainly high-level coupled-cluster ab initio calculations.[1,6,9] These computationally demanding post-Hartree–Fock methods are currently not applicable to systems of the size envisioned here. We thus resort to density functional theory (DFT). To provide a sound methodological basis for our exploration, we recently calibrated different DFT methods in detail against accurate coupled-cluster data for the smaller complexes HgX_4 (X = F, Cl, H).[10] In the absence of experimental data, this theory-against-theory comparison has enabled us to identify exchange-correlation functionals and basis sets that are expected to faithfully reproduce the structures and stabilities of Hg^{IV} complexes. While the structural parameters of Hg^{IV} complexes were best reproduced by the local SVWN and hybrid BHandHLYP functionals, the thermochemistry was best described by hybrid functionals such as B3LYP, B1LYP, and MPW1PW91 that incorporate about 20% Hartree–Fock exchange.[10] Here we use the popular B3LYP functional[16,17] (implementation as in the Gaussian program package,[18] as requested by the keyword b3-lyp Gaussian in the Turbomole program suite[19] used in this study). The comparison in Table 1[10] shows that B3LYP with the basis used in the present work (see below) provides only slightly more endothermic elimination energies than the much more involved CCSD(T) calculations. Similar results were noted for decomposition reactions of high oxidation state compounds in the neighboring Group 11.[20] Note that basis-set convergence for the coupled-cluster results is slower than for DFT, and even larger basis sets than those employed in reference [10] will probably bring the CCSD(T) energetics even closer to the B3LYP data.

Table 1. Comparison of DFT and coupled-cluster elimination, fragmentation and atomization energies [kJ mol^{-1}] for small HgX_4 and HgX_2 (X = F, Cl, H) complexes.[a]

System	B3LYP[b]	CCSD(T)
$HgF_4 \rightarrow HgF_2 + F_2$	+44.0 (+36.3)	+34.0 (+22.7)[c]
$HgCl_4 \rightarrow HgCl_2 + Cl_2$	−133.1 (−134.2)	−156.4 (−165.5)[c]
$HgH_4 \rightarrow HgH_2 + H_2$	−195.5 (−199.4)	−181.4 (−195.6)[b]
$HgF_4 \rightarrow Hg + 4F$	+779.7 (+761.4)	+719.8 (+693.0)[c]
$HgCl_4 \rightarrow Hg + 4Cl$	+530.4 (+521.2)	+522.8 (+501.6)[c]
$HgH_4 \rightarrow Hg + 4H$	+651.6 (+644.1)	+648.4 (+619.8)[b]
$HgF_2 \rightarrow Hg + 2F$	+583.6 (+574.1)	+528.1 (+515.1)[b]
$HgCl_2 \rightarrow Hg + 2Cl$	+461.1 (+454.1)	+442.0 (+431.6)[b]
$HgH_2 \rightarrow Hg + 2H$	+387.2 (+383.7)	+373.0 (+358.7)[b]
$HgF_4 \rightarrow HgF_2 + 2F$	+196.0 (+187.2)	+191.6 (+179.1)[c]
$HgCl_4 \rightarrow HgCl_2 + 2Cl$	+69.4 (+63.9)	+80.8 (+78.8)[c]
$HgH_4 \rightarrow HgH_2 + 2H$	+295.6 (+264.9)	+275.4 (+261.2)[b]

[a] See reference [10]. B3LYP/basis-B and CCSD(T)/basis-A results. [b] Results with CP corrections in parentheses. [c] Results with CCSD/basis-A CP corrections in parentheses.

We use a pseudopotential/basis set combination based on that labeled basis-B in reference [10]. This basis set was found to provide excellent structures and energetics. In particular, it exhibited very small basis-set superposition errors in DFT calculations (cf. Table 1). A quasirelativistic small-core 20-valence-electron pseudopotential[21] (effective core potential, ECP) was used for Hg, with a (8s8p7d2f)/[6s6p4d2f] valence basis set including two uncontracted f functions with exponents $\alpha = 1.5, 0.5$. Quasirelativistic large-core ECPs were used for Al, As, Sb, Se, and Te.[22] The (4s4p)/[2s2p] valence basis sets[22] for Al, As, and Sb were augmented by one polarization d function (see reference [23] for Al and reference [24] for the other atoms) to arrive at basis sets of DZP valence quality. For Se and Te, (4s5p)/[2s3p] valence basis sets[22] were augmented by one diffuse s function (obtained by dividing the smallest s exponent in the 4s set by a factor of three) and one d function,[24] resulting in a DZ+P-quality (5s5p1d)/[3s3p1d] valence basis. In comparative calculations on noble gas compounds, quasirelativistic 8-valence-electron ECPs and (6s6p3d1f)/[4s4p3d1f] valence basis sets were used for Xe and Kr.[25] Fluorine and oxygen were treated at the all-electron level by using Dunning's DZP basis augmented by a diffuse sp set[26] (DZ+P) to give a (10s6p1d)/[5s3p1d] basis. While the valence basis sets on Al, As, Sb, Se, and Te are of slightly lower quality than those for the other atoms, the basis-set incompleteness errors for these "inner" atoms are expected to cancel for the reaction energies studied here. Our previous experience[10] (see Table 1) suggests that the basis sets used exhibit small basis-set superposition errors at the DFT level. Energies will thus be reported without counterpoise (CP) corrections.

All calculations were done with Turbomole 5.6.[19] Structures were fully optimized without symmetry restrictions. Except for a few of the largest systems (complexes of E_2F_{11} ligands and dimers of $Hg(OTeF_5)_2$ and $Hg(OTeF_5)_4$), for which this turned out to be computationally too demanding, minima on the potential energy surface were characterized by harmonic vibrational frequency analyses using numerical second derivatives based on energies and analytical gradients. We provide relative energies without zero-point vibrational corrections, as these do not alter the thermochemistry significantly.[10] Spin–orbit effects were also previously found to be almost negligible for the elimination reactions.[1] Cartesian coordinates of optimized structures and computed vibrational frequencies are available as Supporting Information (Tables S1, S2). Natural population analyses (NPA)[27] were performed with a standalone version of the NBO4.M program,[28] interfaced to Turbomole in our group.[29]

Choice of Ligands

Basically, the idea of using WCAs is equivalent to creating an environment of the metal in the condensed phase that is as close as possible to the gas-phase situation.[14] In particular, we want to avoid high coordination numbers of the Hg^{II} elimination products. Our choice of WCAs was based on 1) their known abilities to stabilize high oxidation states, 2) their experimental availability, and 3) a reasonably moderate size to allow calculation of the complexes at an appropriate theoretical level.

AlF_4^- was chosen as a very small WCA which is expected to provide less stabilization than the larger ligands. It serves mainly for comparison purposes. During the optimizations we saw in some cases formation of the dinuclear Al_2F_7 ligand and therefore include a few complexes of this anion as well. AsF_6^- and SbF_6^- are WCAs that are well known to stabilize unusual cations and high oxidation states, including noble gas species.[14,15] These anions are furthermore known to condense exothermically to the dinuclear anions $Sb_2F_{11}^-$ and $As_2F_{11}^-$,[30] which are supposed to be even more weakly coordinating, as their negative charge is even more delocalized (the trinuclear $[Sb_3F_{16}]^-$ and tetranuclear $[Sb_4F_{21}]^-$ ions are also known[30]), and we included them for comparison. Furthermore, it was interesting to compare $Sb_2F_{11}^-$ with $As_2F_{11}^-$, as the latter tends to be less stable relative to the corresponding mononuclear ligand EF_6^-.

The very potent WCAs $[E(OTeF_5)_6]^-$ (E = As, Sb, Bi, Nb)[14,15,31] were too large for our purposes, given our available computational resources. However, the experimentally known pentafluorooxotellurate ("teflate") anion $OTeF_5^-$ and its selenium homologue $OSeF_5^-$ appeared to be promising ligands. They are often discussed as "bulky fluoride analogues" and are well known to stabilize high oxidation states[31] and unusual cations.[15,31] Their group electronegativities are thought to be comparable to that of fluorine, and they are unlikely to favor high coordination numbers in the Hg^{II} product complexes.[31] These OEF_5^- ligands are also unlikely to favor elimination reactions by condensing to larger units, and they are stable to fluoride abstraction.[15]

In the following section we report structures of the HgX_4 and *cis*- and *trans*-HgF_2X_2 complexes and of their Hg^{II} elimination products, their thermochemical stabilities, and a brief analysis of interrelations between bonding and stability.

Results

Structures

$X^- = AlF_4^-$, $Al_2F_7^-$: The computed structures of *cis*- and *trans*-$HgF_2[AlF_4]_2$ exhibit the expected square-planar primary coordination of low-spin $5d^8$ Hg^{IV}, with slightly shorter Hg–F(F) than Hg–F(AlF_4) distances (Figure 1 b,c). In contrast, the coordination is distorted for $Hg[AlF_4]_4$, with deviations from planarity and unequal primary Hg–F distances (Figure 1 a). The primary coordination is in all three cases augmented by one weaker axial fluorine contact from each AlF_4 ligand (for $Hg[AlF_4]_4$ the primary distances are somewhat longer and the secondary distances shorter than for the other two species). The optimized structures exhibit C_1 symmetry for $Hg[AlF_4]_4$, C_2 symmetry for *cis*-$HgF_2[AlF_4]_2$, and D_{2h} symmetry for *trans*-$HgF_2[AlF_4]_2$. During one structure optimization of the *cis* isomer, an AlF_3 unit was transferred from one of the coordinated AlF_4 ligands to the other to form a coordinated Al_2F_7 ligand. The resulting C_1-symmetrical $HgF_3[Al_2F_7]$ has one weak axial contact from a fluorine atom of the Al_2F_7 ligand in form of a six-membered chelate ring (Figure 1 d). This complex is about 62.3 kJ mol^{-1} more stable than *cis*-$HgF_2[AlF_4]_2$, which in turn is 5.4 kJ mol^{-1} more stable than its *trans* isomer. The condensed binuclear ligand thus appears to provide an energy sink in these systems. This led us to consider also HgF_2-$[Al_2F_7]_2$. In the optimized, nonsymmetric structure (Fig-

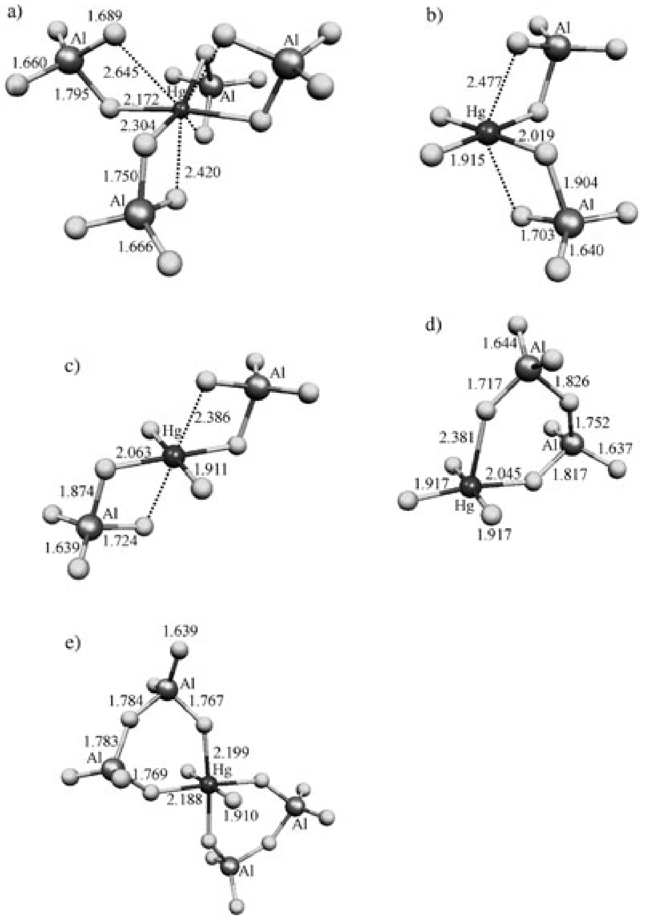

Figure 1. Optimized structures for Hg^{IV} complexes with AlF_4 or Al_2F_7 ligands: a) $Hg(AlF_4)_4$; b) *cis*-$HgF_2(AlF_4)_2$; c) *trans*-$HgF_2(AlF_4)_2$; d) $HgF_3(Al_2F_7)$; e) $HgF_2(Al_2F_7)_2$.

ure 1e), each $[Al_2F_7]^-$ ligand coordinates to two equatorial positions in a compressed octahedron, and the terminal fluoro ligands occupy the axial positions.

Possible elimination products for these systems include the Hg^{II} complex $Hg(AlF_4)_2$, which exhibits D_{2d} symmetry and tetrahedral mercury coordination due to bidentate binding of both ligands (Figure 2a). The most stable structure found for $Hg(Al_2F_7)_2$ (C_2 symmetry) exhibits a bidentate chelate binding mode of the dinuclear ligand and also tetrahedral coordination of Hg (Figure 2b).

$X^- = EF_6^-$ (E = As, Sb): Figure 3 shows square-planar primary coordination to mercury in all Hg^{IV} complexes, augmented by two further, weaker axial contacts (four in the case of $Hg(SbF_6)_4$; Figure 3b). Primary Hg–F distances to the EF_6 ligands tend to be in the 1.95–1.96 Å range, shorter than the 2.05–2.06 Å for AlF_4 ligands (cf. Figure 1) but slightly longer than the distances to fluoride. In contrast, the secondary contacts range from 2.59 to 2.77 Å, considerably longer than the 2.38–2.39 Å of the aluminum systems. This indicates a lower tendency towards bidentate bonding.

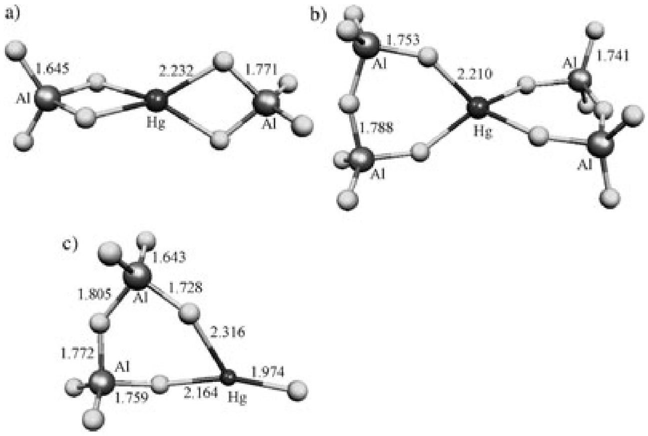

Figure 2. Optimized structures for Hg^{II} complexes with AlF_4 or Al_2F_7 ligands: a) $Hg(AlF_4)_2$; b) $Hg(Al_2F_7)_2$; c) $HgF(Al_2F_7)$.

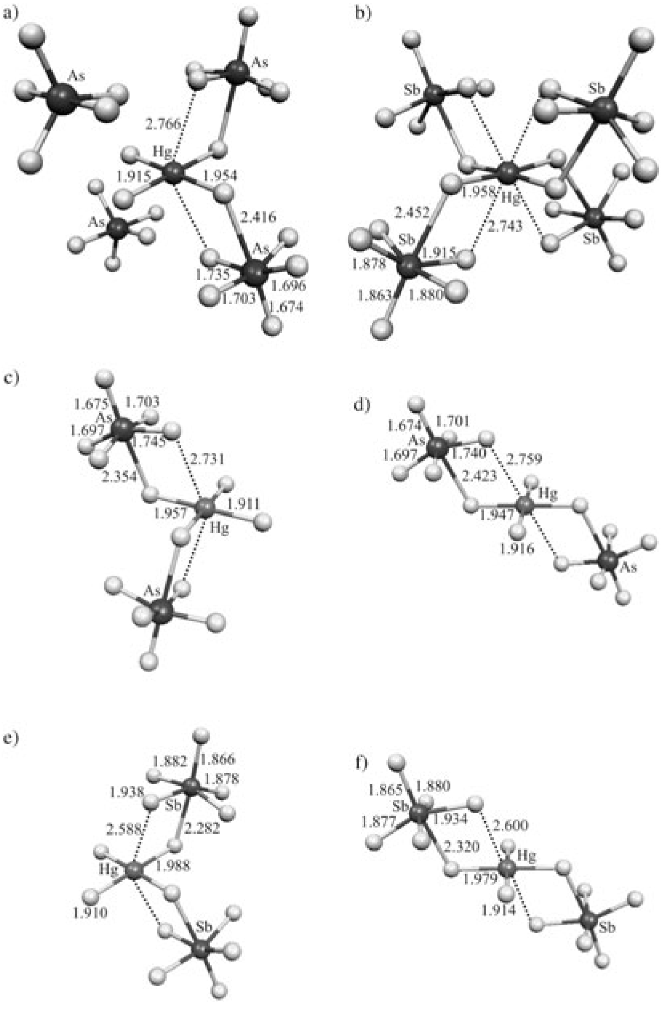

Figure 3. Optimized structures for Hg^{IV} complexes with AsF_6 or SbF_6 ligands. a) $Hg(AsF_6)_4$; b) $Hg(SbF_6)_4$; c) *cis*-$HgF_2(AsF_6)_2$; d) *trans*-$HgF_2(AsF_6)_2$; e) *cis*-$HgF_2(SbF_6)_2$; f) *trans*-$HgF_2(SbF_6)_2$.

In all bound octahedral EF_6 ligands, the E–F bond to the coordinating fluorine atom is lengthened substantially compared to the other bonds in the ligand, and the equatorial fluorine atoms are bent towards the fluorine atom that coordinates to mercury. This indicates substantial weakening of the metal-coordinated E–F bond in all cases (as a consequence, the E–F bond in the *trans* position is shortened). Indeed, optimization of $Hg(AsF_6)_4$ led to dissociation of two AsF_5 molecules from two AsF_6 ligands in *cis* position, leading to *cis*-$HgF_2(AsF_6)_2$ with two loosely attached AsF_5 molecules (Figure 3a, cf. the very similar structural parameters of free *cis*-$HgF_2(AsF_6)_2$, Figure 3c). This seems to be a relatively general observation for the arsenium-based systems (see below). In contrast, all four SbF_6 ligands stay intact in $Hg(SbF_6)_4$ (Figure 3b; the structure has C_2 symmetry), but the F–Sb bond of the coordinated fluorine is lengthened substantially.

The greater resistance of the SbF_6 ligands towards loss of SbF_5 (see below for the associated energetics) may also be discerned in the other cases from the somewhat less pronounced lengthening of the E–F bonds involved in metal coordination (see Figure 3c versus 3e for *trans*-$HgF_2(EF_6)_2$ and Figure 3d versus 3f for the *cis* complexes). In general, equatorial E–F bonds involved in secondary coordination to mercury are lengthened more moderately, as one might expect. Owing to the less pronounced extension of the E–F bond to the coordinated fluorine atom in the $HgF_2(EF_6)_2$ systems compared to $Hg(EF_6)_4$, we can consider the AsF_6 ligands to still be intact in these complexes (Figure 3c,d). The *cis* isomers of $HgF_2(AsF_6)_2$ and $HgF_2(SbF_6)_2$ are more stable than the *trans* isomers by about 4 and about 10 kJ mol^{-1}, respectively. This may be interpreted as a slightly larger *trans* influence of free fluoride compared to EF_6^-.

In view of the discussion in the introduction regarding aggregation of the Hg^{II} elimination products, the structures of the $Hg(EF_6)_2$ complexes are of particular interest. As shown in Figure 4, these both exhibit almost regular octahedral coordination to mercury (the complexes have D_{3d} symmetry), whereby three fluorine atoms on one face of each EF_6 unit bind to the metal in a tridentate fashion. While the computed Hg–F distances are significantly longer than that of a full single bond (ca. 2.0 Å), the relatively high coordination number is notable (see below). The E–F bond lengths of the coordinated fluorine atoms are significantly elongated, but much less so than the single coordinating E–F bond in the Hg^{IV} complexes (cf. Figure 3). The AsF_6 ligand is much less distorted than in the Hg^{IV} case. Together, these observations indicate three moderate Hg–F bonding interactions to each ligand.

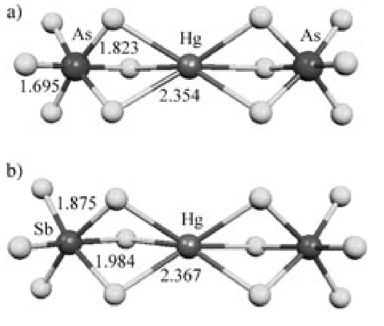

Figure 4. Optimized structures for Hg^{II} complexes with AsF_6 or SbF_6 ligands: a) $Hg(AsF_6)_2$; b) $Hg(SbF_6)_2$.

$X^- = E_2F_{11}^-$ (E = As, Sb): Optimized structures of Hg^{IV} complexes with the dinuclear E_2F_{11} ligands are shown in Figure 5. Optimization of $Hg(As_2F_{11})_4$ leads to dissociation of AsF_5 from all four ligands to form a system best described as $Hg(AsF_6)_4{\cdot}4\,AsF_5$ (Figure 5a; cf. the structure of $Hg(AsF_6)_4$ in Figure 3a), or maybe even as $HgF_4{\cdot}8\,AsF_5$. We were not able to locate a stable minimum for $Hg(Sb_2F_{11})_4$. In one optimization, spontaneous reductive elimination of F_2 occurred with formation of $Hg(Sb_2F_{11})_2 + 2\,SbF_5$. In another optimization, Sb_2F_{10} was extruded with formation of $HgF(Sb_2F_{11})_3$ (Figure 5b). This does not necessarily mean that $Hg(Sb_2F_{11})_4$ does not exist, but the size of the system prevented us from more extensive searches for a minimum structure. In any case it seems that there is not much gain in stability on going from the SbF_6 to the Sb_2F_{11} ligand, or from $HgF_2(Sb_2F_{11})_2$ to $Hg(Sb_2F_{11})_4$ (see below).

Minima were found for the $HgF_2[E_2F_{11}]_2$ complexes. The structures also differ appreciably between E = As and E =

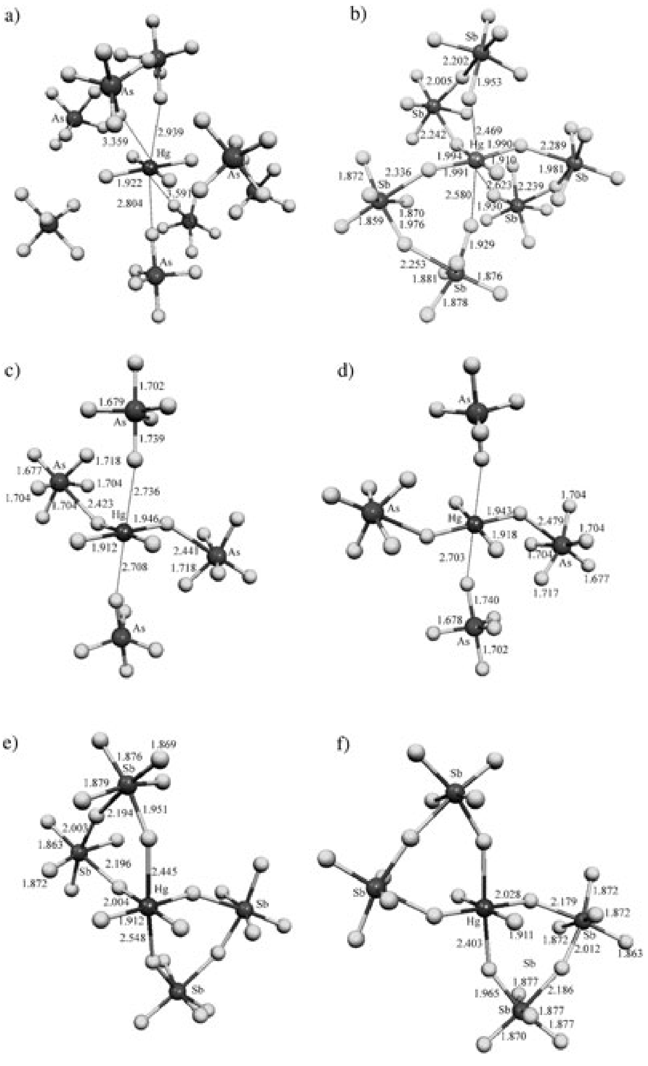

Figure 5. Optimized structures for Hg^{IV} complexes with As_2F_{11} or Sb_2F_{11} ligands: a) $HgF_4{\cdot}8\,AsF_5$; b) $HgF(Sb_2F_{11})_3$; c) *cis*-$HgF_2(AsF_6)_2{\cdot}2\,AsF_5$; d) *trans*-$HgF_2(AsF_6)_2{\cdot}2\,AsF_5$; e) *cis*-$HgF_2(Sb_2F_{11})_2$; f) *trans*-$HgF_2(Sb_2F_{11})_2$.

Sb (Figure 5c–f). In the case of E = As, again two AsF_5 units dissociate and are only loosely connected to the remaining AsF_6 ligand, so that both *cis* and *trans* complexes essentially become $HgF_2(AsF_6)_2 \cdot 2\,AsF_5$ (Figure 5c,e), similar to the result of structure optimization of $Hg[AsF_6]_4$ (see above), and with the same stoichiometric composition. In contrast to the latter case, where the AsF_5 units are closest to metal-bound fluoride (cf. Figure 3a), here they are bound very weakly to an axial fluorine atom of the AsF_6 ligand (*trans* to mercury). While the two structures are also minima, the binding is slightly less favorable in the latter case, and the *cis* complex in Figure 5c is about 8 $kJ\,mol^{-1}$ less stable than the arrangement in Figure 3a. The *trans* complex (Figure 5e) is a further 4 $kJ\,mol^{-1}$ less stable. For $HgF_2[Sb_2F_{11}]_2$, the *cis* isomer is also about 8 $kJ\,mol^{-1}$ more stable than the *trans* isomer (see also above). Here the dinuclear ligands remain intact (but with unsymmetrical F-E-F bridges), and the Sb_2F_{11} ligands bend around to allow secondary contacts to mercury by the "remote" SbF_5 groups (this appears to be preferable to bidentate bonding from fluorine atoms attached to the same Sb center, as found for the SbF_6 complexes; cf. Figure 3). The somewhat unsymmetrical bridges are similar to those found in the solid state or, for example, in ab initio molecular dynamics studies on liquid SbF_5 or $HF \cdot SbF_5$ solutions.[32]

The Hg^{II} products of reductive F_2 elimination, $Hg(E_2F_{11})_2$, have C_i symmetry (Figure 6). As for the complexes $Hg(EF_6)_2$ above, the coordination of mercury is distorted octahedral. However, now only two of the three bonding contacts of each ligand derive from one chelate-bonded EF_6 unit, whereas the second EF_5 unit bends around to provide a third, slightly shorter contact in a chelating fashion (six-membered ring). Notably, the As_2F_{11} ligands remain intact in this case, in contrast to the Hg^{IV} species in Figure 5 (Sb-F-Sb bridges in the Sb_2F_{11} ligands are also somewhat more symmetrical than in the Hg^{IV} case).

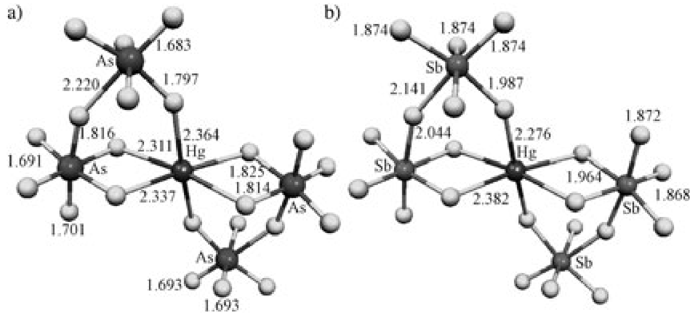

Figure 6. Optimized structures for Hg^{II} complexes with As_2F_{11} or Sb_2F_{11} ligands: a) $Hg(As_2F_{11})_2$; b) $Hg(Sb_2F_{11})_2$.

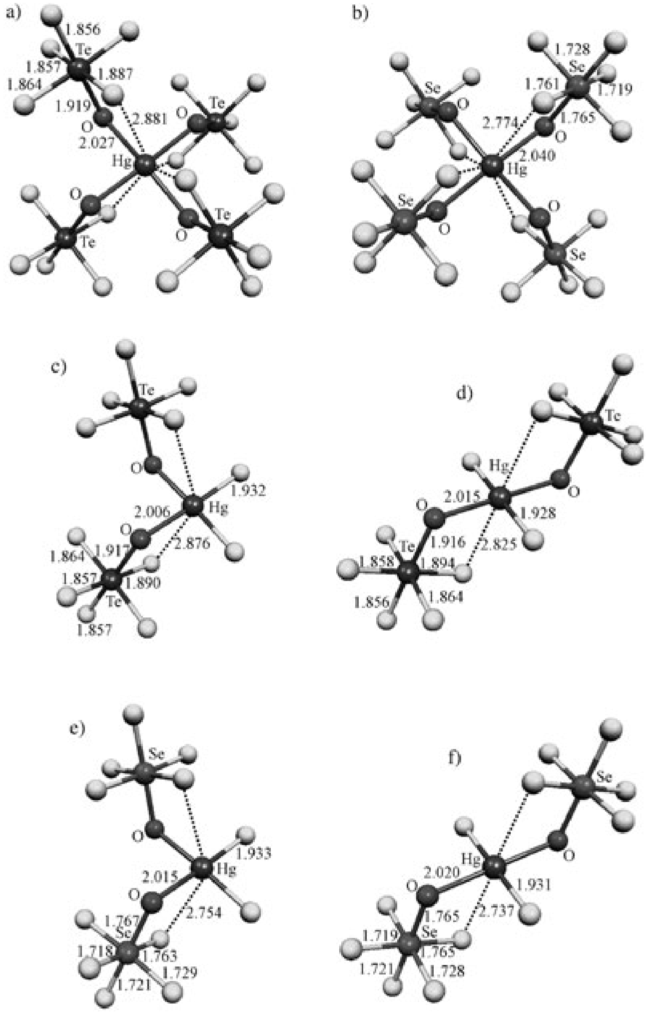

Figure 7. Optimized structures for Hg^{IV} complexes with OEF_5 ligands: a) $Hg(OTeF_5)_4$; b) $Hg(OSeF_5)_4$; c) *cis*-$HgF_2(OTeF_5)_2$; d) *trans*-$HgF_2(OTeF_5)_2$; e) *cis*-$HgF_2(OSeF_5)_2$; f) *trans*-$HgF_2(OSeF_5)_2$.

$X^- = OEF_5^-$ (E = Se, Te): The optimizations produce structures of relatively high symmetry (D_{2d}) for $Hg(OEF_5)_4$ (Figure 7a,b). The *trans*-$HgF_2(OEF_5)_2$ complexes exhibit C_{2h} symmetry (Figure 7d,f), and the *cis* complexes C_2 symmetry (Figure 7c,e). As expected,[31] the OEF_5 ligands coordinate primarily through their oxygen atom (Hg–O 2.01–2.04 Å) and thus form square-planar HgO_4- or HgF_2O_2-type primary coordination. Secondary interactions again involve one equatorial fluorine atom of each ligand. Distances of these secondary interactions tend to be between 2.74 and 2.88 Å, longer than in the previously discussed systems (similar weak axial secondary M···F contacts were found by X-ray crystallography in dimeric square-planar $Au(OTeF_5)_3$[33]). The Hg-O-E angles are similar in all complexes, close to 118.0°. This is smaller than the typical values of about 125–135° found for other coordinated OEF_5 anions[15,31] but similar to the values found for $[Au(OTeF_5)_3]_2$,[33] consistent with the presence of secondary M···F contacts. The computed D_{2d} structure for $Hg(OTeF_5)_4$ is similar to the experimentally determined X-ray structure of $Xe(OTeF_5)_4$,[34] except for a few details: 1) the secondary axial Xe···F contacts are much longer (ca. 3.2 Å, Xe-O-Te angles are ca. 130°) than the optimized Hg···F contacts; 2) the orientation of the $OTeF_5$ ligands in $Xe(OTeF_5)_4$ was found to be up-up-down-down

(C_{2h}), in contrast to the more intuitive up-down-up-down alternating structure favored for the mercury complex (cf. Figure 7a). The latter point appears to be due to packing effects in the solid for the xenon compound.[34] Our optimizations of $Xe(OTeF_5)_4$ (see Table S1 in Supporting Information for optimized coordinates) favor the alternating D_{2d} arrangement over the nonalternating C_{2h} one by about 10 kJ mol^{-1}.

The somewhat longer primary Hg–F bonds in the *cis*- compared to the *trans*-$HgF_2(OEF_5)_2$ complexes reflect a slightly larger *trans* influence of the OEF_5 ligand compared to fluoride (whereas the Hg–O distances are somewhat longer in the *trans* complexes). The *cis* isomer of $HgF_2(OTeF_5)_2$ is slightly (ca. 6 kJ mol^{-1}) more stable than the *trans* complex, in contrast to the other systems discussed above. The *trans* isomer of the $OSeF_5$ complex is favored marginally (by ca. 1.1 kJ mol^{-1}). These results confirm that electronegativity and *trans* influence of the OEF_5 anions are similar to those of the fluoride ion[31] (but see below for differences). This makes these ligands particularly attractive.

In contrast to the EF_6 ligands, the angles in the OEF_5 ligands are all close to ideal octahedral, as is well known for the coordinated ligand[31] (in the free anions, the O-E-F_{eq} angles tend to be closer to 95°[35]). A slight lengthening of E–F distances for equatorial fluorine atoms involved in secondary coordination to mercury is again apparent (see above). The other equatorial E–F bond lengths are similar to that of the axial bond *trans* to oxygen. This reflects a reduction of the *trans* influence of the oxygen atom within the ligand, due to its involvement in bonding to mercury. Structures of the $OSeF_5$ and $OTeF_5$ complexes are very similar, apart from the naturally shorter E–F and E–O bonds in the selenium systems. Dimensions within the ligands agree well with those of known structures.[15,31]

Computed structures for the C_{2h}-symmetrical Hg^{II} complexes obtained after F_2 elimination are shown in Figure 8. Notably, the coordination of mercury is not sixfold as with EF_6 or E_2F_{11} ligands, but effectively fourfold: two primary bonds from the oxygen atoms of the two OEF_5 ligands are supplemented by substantially weaker secondary bonds from equatorial fluorine atoms of the ligands (the two secondary bonds are oriented mutually *trans* and thus render the overall metal coordination planar). Notably, the primary bond is slightly shorter for E = Te, whereas the secondary contact is appreciably longer. Interestingly, the secondary $Hg^{II}\cdots F$ interactions have distances that do not differ much from those seen in the Hg^{IV} complexes (cf. Figure 7).

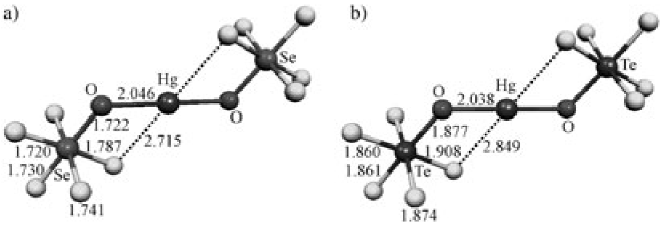

Figure 8. Optimized structures for Hg^{II} complexes with OEF_5 ligands: a) $Hg(OSeF_5)_2$; b) $Hg(OTeF_5)_2$.

The other primary products of X_2 elimination from HgX_4 or of F_2 elimination from HgF_2X_2 are the peroxidic dimers $(OEF_5)_2$, shown in Figure 9. They exhibit C_2 symmetry with an E-O-O-E dihedral angle of 118.5°, similar to the parent compound hydrogen peroxide. The O–O bond is somewhat shorter for the selenium system. The O–O distances in both systems are shorter than the computed O–O bond length of H_2O_2 at the same level (1.453 Å). Experimental O–O bond lengths are 1.45 ± 4 and 1.48 ± 0.01 Å for $F_5TeOOTeF_5$[36] and H_2O_2,[37] respectively. It has been argued that the O–O bonds in the F_5EO–OEF_5 derivatives are made particularly strong by the electron-withdrawing nature of the EF_5 substituents.[31] However, as we will show below, this is not the case.

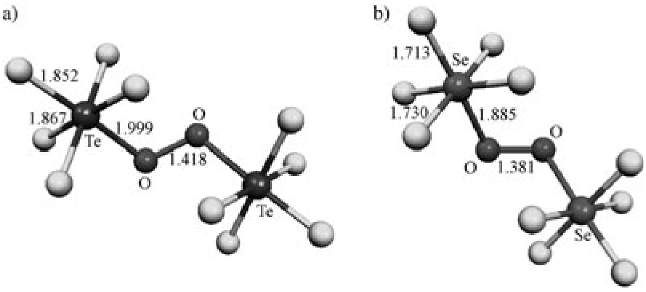

Figure 9. Optimized structures for peroxide species $(OTeF_5)_2$ and $(OSeF_5)_2$: a) $(OTeF_5)_2$; b) $(OSeF_5)_2$.

Thermochemical stability of Hg^{IV} versus Hg^{II} complexes

The most important decomposition channels towards which the Hg^{IV} complexes may be unstable are 1) elimination of F_2, and 2) elimination of X_2 (where possible). Elimination of FX was not explicitly considered, as the energies of this reaction are expected to be intermediate between those of the other two routes. We thus investigated energies of the reactions $HgF_2X_2 \rightarrow HgX_2 + F_2$ and $HgF_2X_2 \rightarrow HgF_2 + X_2$. The latter pathway is only viable for X = OEF_5 (E = Se, Te), as the X_2 elimination products are unfavorable in the other cases. Elimination of F_2 may in some cases be followed in principle by subsequent reactions, for example, $Hg(EF_6)_2 \rightarrow HgF_2 + 2EF_5$ (E = As, Sb). As these reactions are relevant to the overall competitiveness of a given set of ligands, we also consider them. For the HgX_4 complexes, the reaction $HgX_4 \rightarrow HgX_2 + X_2$ is expected to be competitive only for OEF_5 ligands. In all other cases, F_2 elimination with ligand fragmentation is expected to be the dominant decomposition channel, for example, as $Hg(EF_6)_4 \rightarrow Hg(EF_6)_2 + (EF_5)_2 + F_2$ (E = As, Sb).

$X^- = AlF_4^-$, $Al_2F_7^-$: As shown in Table 2, $Hg(AlF_4)_4$ is rather unfavorable thermochemically. In addition to exo-

Table 2. Computed reaction energies [kJ mol^{-1}] for complexes with AlF_4 and Al_2F_7 ligands.

Reaction	Structure	ΔE
$Hg(AlF_4)_4 \rightarrow Hg(AlF_4)_2 + (AlF_3)_2 + F_2$		−180.5
$Hg(AlF_4)_4 \rightarrow Hg(Al_2F_7)_2 + F_2$		−307.0
$HgF_2(AlF_4)_2 \rightarrow Hg(AlF_4)_2 + F_2$	*trans*	−106.3
$HgF_2(AlF_4)_2 \rightarrow Hg(AlF_4)_2 + F_2$	*cis*	−100.9
$HgF_2(AlF_4)_2 \rightarrow HgF(Al_2F_7) + F_2$	*trans*	−93.4
$HgF_2(AlF_4)_2 \rightarrow HgF(Al_2F_7) + F_2$	*cis*	−88.0
$HgF_3(Al_2F_7) \rightarrow HgF(Al_2F_7) + F_2$		−25.6
$HgF_3(Al_2F_7) \rightarrow Hg(AlF_4)_2 + F_2$		−38.5
$HgF_2(Al_2F_7)_2 \rightarrow Hg(Al_2F_7)_2 + F_2$		−126.0
$Hg(AlF_4)_2 \rightarrow HgF_2 + (AlF_3)_2$		+129.2
$Hg(Al_2F_7)_2 \rightarrow HgF_2 + 2\ (AlF_3)_2$		+255.7
$HgF(Al_2F_7) \rightarrow HgF_2 + (AlF_3)_2$		+116.3
$(AlF_3)_2 \rightarrow 2\ AlF_3$		+188.7

thermic F_2 elimination accompanied by ligand fragmentation, an even more exothermic channel involves attachment of intermediately formed AlF_3 entities to the initial elimination product $Hg(AlF_4)_2$ to form the more stable $Hg(Al_2F_7)_2$. We have not identified such extremely exothermic decomposition pathways for the $HgF_2(AlF_4)_2$ isomers. Interestingly, the rearrangement product $HgF_3(Al_2F_7)$ is about 60–70 kJ mol^{-1} more stable than the latter complexes (see above and Figure 1). However, it appears an unlikely species to be formed in a superacidic condensed-phase environment. $HgF_2(Al_2F_7)_2$ also decomposes exothermically.

$X^- = EF_6^-$ (M = As, Sb): Table 3 summarizes reaction energies for the $Hg(EF_6)_4$ and $HgF_2(EF_6)_2$ complexes. While all species are again thermochemically unstable towards elimination of F_2, the reaction energies are in the range from −60 to −120 kJ mol^{-1}. The more favorable cases are thus less endothermic than the AlF_4 or Al_2F_7 complexes. The *cis*-$HgF_2(EF_6)_2$ complexes are marginally more stable than their *trans* isomers (see above). Interestingly, the AsF_6 complexes tend to be less endothermic than their SbF_6 analogues, in spite of the ready removal of AsF_5 from AsF_6 ligands bound to Hg^{IV}. This has to do with the fact that the strongly endothermic fragmentation of the $Hg(EF_6)_2$ elimination product into HgF_2 and EF_5 is energetically much more costly for E = Sb than for E = As. Indeed, the less favorable thermochemistry relative to gas-phase HgF_4 may also be viewed as a consequence of the stronger binding of EF_5 in the Hg^{II} species compared to the Hg^{IV} complexes. As this differential effect (Table 3) is more pronounced with SbF_6 ligands, the Hg^{IV} complexes with AsF_6 ligands exhibit a more favorable thermochemistry. This becomes even more pronounced when we consider that SbF_5 has a much larger tendency to aggregate than AsF_5 (cf. dimerization energies for EF_5 in Table 3). Indeed, SbF_5 is an oil at room temperature (m.p. 8.3 °C, b.p. 141 °C), with polymeric zigzag chains of *cis*-interlinked octahedra.[30] It forms tetramers in the solid-state. In the gas phase at 252 °C, dimers dominate.[30] Already when we take into account the dimerization energy of SbF_5 in computing the elimination energies (values in parentheses in Table 3), the Hg^{IV} complexes with SbF_6 ligands become still more unfavorable. Many of them are probably not competitive in the condensed phase.

Table 3. Computed reaction energies [kJ mol^{-1}] for complexes with EF_6 ligands (E = As, Sb).

Reaction	Structure	ΔE
$Hg(AsF_6)_4 \rightarrow Hg(AsF_6)_2 + 2\,AsF_5 + F_2$		−61.4[a]
$Hg(SbF_6)_4 \rightarrow Hg(SbF_6)_2 + 2\,SbF_5 + F_2$		−85.9 (−160.9)[b]
$HgF_2(AsF_6)_2 \rightarrow Hg(AsF_6)_2 + F_2$	*cis*	−76.1
	trans	−76.8
$HgF_2(SbF_6)_2 \rightarrow Hg(SbF_6)_2 + F_2$	*cis*	−110.5
	trans	−120.0
$Hg(AsF_6)_4 \rightarrow HgF_4 + 4\,AsF_5$		+44.0[a]
$Hg(SbF_6)_4 \rightarrow HgF_4 + 4\,SbF_5$		+115.5 (−34.5)[b]
$HgF_2(AsF_6)_2 \rightarrow HgF_4 + 2\,AsF_5$	*cis*	+29.3
	trans	+25.2
$HgF_2(SbF_6)_2 \rightarrow HgF_4 + 2\,SbF_5$	*cis*	+91.5 (+16.5)[b]
	trans	+82.0 (+6.0)[b]
$Hg(AsF_6)_2 \rightarrow HgF_2 + 2\,AsF_5$		+150.6
$Hg(SbF_6)_2 \rightarrow HgF_2 + 2\,SbF_5$		+247.2 (+172.2)[b]
$As_2F_{10} \rightarrow 2\,AsF_5$		−19.6[c]
$Sb_2F_{10} \rightarrow 2\,SbF_5$		+75.0[c]

[a] See $HgF_2(AsF_6)_2 \cdot 2\,AsF_5$-type structure for $Hg(AsF_6)_4$ in Figure 3a. [b] Values in parentheses obtained after taking into account dimerization of SbF_5. [c] MP2 values are +13.2 kJ mol^{-1} and +109.9 kJ mol^{-1} for As_2F_{10} and Sb_2F_{10}, respectively.

In contrast, AsF_5 shows little tendency to aggregate. At the B3LYP level, As_2F_{10} is unbound. This may arise from a poor description of dispersion interactions by the DFT method used. MP2 calculations provide larger binding energies for both As_2F_{10} and Sb_2F_{10} (cf. Table 3) but confirm that the aggregation energy of AsF_5 is indeed very small. At room temperature, AsF_5 is a monomeric gas (m.p. −79.8 °C, b.p. −52.8 °C).[30] This lack of aggregation is favorable for the stability of the Hg^{IV} complexes with AsF_6 ligands. While AsF_5 is split off relatively easily from the Hg^{IV} complexes, and less so for $Hg(AsF_6)_2$, the associated differential energy effect is less pronounced than for SbF_6 ligands (Table 3). Moreover, there is little extra energetic penalty provided by aggregation of the elimination products. This makes complexes like $HgF_2(AsF_6)_2$ or $Hg(AsF_6)_4$ good candidates for mercury(IV) chemistry.

$X^- = E_2F_{11}^-$ (E = As, Sb): The trends discussed for the EF_6 ligands become even more pronounced for the dinuclear E_2F_{11} ligands (Table 4). We did not find a stable minimum for $Hg(Sb_2F_{11})_4$, and $Hg(As_2F_{11})_4$ is essentially HgF_4 with only loosely connected AsF_5 units (cf. Figure 5a). The ready extrusion of AsF_5 from As_2F_{11} ligands bound to Hg^{IV} is apparent (Table 4). Table 4 also contains data for the free E_2F_{11} anions. Together, these data indicate that the energy cost of removing an AsF_5 ligand from an As_2F_{11} unit is about +20–25 kJ mol^{-1} when the ligand is bound to Hg^{IV}, about +55–60 kJ mol^{-1} in $Hg^{II}(As_2F_{11})_2$, and about +78 kJ mol^{-1} in the free anion. The corresponding values for Sb_2F_{11} ligands are about +107, about +167, and about +130 kJ mol^{-1}, respectively (Table 4). This indicates on the one hand that the antimony systems are held together more tightly, consistent with the higher Lewis acidity of SbF_5 com-

Table 4. Computed reaction energies [$kJ\,mol^{-1}$] for complexes with E_2F_{11} ligands (E = As, Sb).

Reaction	Structure	ΔE
$Hg(As_2F_{11})_4 \rightarrow Hg(As_2F_{11})_2 + 4\,AsF_5 + F_2$		-83.6[a]
$HgF(Sb_2F_{11})_3 \rightarrow Hg(Sb_2F_{11})_2 + F_2 + 2\,SbF_5$		-128.5 (-203.5)[b]
$HgF_2(As_2F_{11})_2 \rightarrow Hg(As_2F_{11})_2 + F_2$	*cis*	-109.7[c]
	trans	-111.4[c]
$HgF_2(Sb_2F_{11})_2 \rightarrow Hg(Sb_2F_{11})_2 + F_2$	*cis*	-171.1
	trans	-180.3
$Hg(As_2F_{11})_4 \rightarrow HgF_2(As_2F_{11})_2 + 4\,AsF_5$	*cis*	$+26.1$[a],[c]
	trans	$+27.8$[a],[c]
$Hg(As_2F_{11})_4 \rightarrow HgF_4 + 8\,AsF_5$		$+78.5$[a]
$HgF_2(As_2F_{11})_2 \rightarrow HgF_2(AsF_6)_2 + 2\,AsF_5$	*cis*	$+23.1$[c]
	trans	$+25.5$[c]
$HgF_2(Sb_2F_{11})_2 \rightarrow HgF_2(SbF_6)_2 + 2\,SbF_5$	*cis*	$+107.0$ ($+32.0$)[b]
	trans	$+107.3$ ($+32.3$)[b]
$Hg(As_2F_{11})_2 \rightarrow Hg(AsF_6)_2 + 2\,AsF_5$		$+56.8$
$Hg(Sb_2F_{11})_2 \rightarrow Hg(SbF_6)_2 + 2\,SbF_5$		$+167.6$ ($+92.8$)[b]
$As_2F_{11}^- \rightarrow AsF_6^- + AsF_5$		$+78.5$
$Sb_2F_{11}^- \rightarrow SbF_6^- + SbF_5$		$+130.5$

[a] See Figure 5a for the "$HgF_4{\cdot}8\,AsF_5$-type" structure of $Hg(As_2F_{11})_4$. [b] Values in parentheses obtained after taking into account dimerization of SbF_5 (cf. Table 3). [c] See Figure 5c,d for the "$Hg(AsF_6)_2{\cdot}2\,AsF_5$-type" structure of $HgF_2(As_2F_{11})_2$.

Table 5. Computed reaction energies [$kJ\,mol^{-1}$] for complexes with OEF_5 ligands (E = Se, Te).

Reaction	Structure	ΔE
$Hg(OSeF_5)_4 \rightarrow Hg(OSeF_5)_2 + (OSeF_5)_2$		-131.8
$Hg(OTeF_5)_4 \rightarrow Hg(OTeF_5)_2 + (OTeF_5)_2$		-121.7
$HgF_2(OSeF_5)_2 \rightarrow (OSeF_5)_2 + HgF_2$	*cis*	-111.3
	trans	-110.5
$HgF_2(OTeF_5)_2 \rightarrow (OTeF_5)_2 + HgF_2$	*cis*	-98.4
	trans	-103.4
$HgF_2(OSeF_5)_2 \rightarrow Hg(OSeF_5)_2 + F_2$	*cis*	$+21.5$
	trans	$+22.3$
$HgF_2(OTeF_5)_2 \rightarrow Hg(OTeF_5)_2 + F_2$	*cis*	$+21.4$
	trans	$+16.5$
$(OSeF_5)_2 \rightarrow 2\,{}^{\bullet}OSeF_5$		$+170.8$
$(OTeF_5)_2 \rightarrow 2\,{}^{\bullet}OTeF_5$		$+182.2$
$H_2O_2 \rightarrow 2\,{\cdot}OH$		$+212.4$[a]
$F_2 \rightarrow 2\,{}^{\bullet}F$		$+154.1$[b]
$Hg(OSeF_5)_4 \rightarrow Hg(OSeF_5)_2 + 2\,{}^{\bullet}OSeF_5$		$+39.0$
$Hg(OTeF_5)_4 \rightarrow Hg(OTeF_5)_2 + 2\,{}^{\bullet}OTeF_5$		$+60.4$
$Hg(OSeF_5)_4 \rightarrow Hg + 4\,{}^{\bullet}OSeF_5$		$+507.5$
$Hg(OTeF_5)_4 \rightarrow Hg + 4\,{}^{\bullet}OTeF_5$		$+553.2$
$HgF_2(OSeF_5)_2 \rightarrow Hg(OSeF_5)_2 + 2\,{}^{\bullet}F$	*cis*	$+175.7$
	trans	$+176.5$
$HgF_2(OTeF_5)_2 \rightarrow Hg(OTeF_5)_2 + 2\,{}^{\bullet}F$	*cis*	$+175.7$
	trans	$+170.7$
$HgF_2(OSeF_5)_2 \rightarrow HgF_2 + 2\,{}^{\bullet}OSeF_5$	*cis*	$+59.5$
	trans	$+60.3$
$HgF_2(OTeF_5)_2 \rightarrow HgF_2 + 2\,{}^{\bullet}OTeF_5$	*cis*	$+83.7$
	trans	$+78.8$

[a] Experimental value 199.8 $kJ\,mol^{-1}$, cf. L. P. Lindeman, J. C. Guffy, *J. Chem. Phys.* **1958**, *29*, 247. [b] Experimental value 154.2 $kJ\,mol^{-1}$, see: K. P. Huber, G. Herzberg, *Molecular Spectra and Molecular Structure. IV. Constants of Diatomic Molecules*, Van Nostrand Reinhold, New York, **1979**.

pared to AsF_5[14] (cf. also dimerization energies of EF_5 in Table 3). Indeed, the As_2F_{11} unit is less well known and characterized than its Sb analogue.[38] On the other hand, differential binding effects within the E_2F_{11} ligands will particularly favor the Hg^{II} complexes and thus disfavor the Hg^{IV} complexes (Table 4). This has to do with the more ionic bonding in the Hg^{II} compared to the Hg^{IV} complexes, which gives rise to less destabilization of the *trans* E–F bonds in the coordinated ligands (see bonding analysis below).

As EF_5 units are thus bound much more loosely in $Hg(E_2F_{11})_4$ or $HgF_2(E_2F_{11})_2$ than in $Hg(E_2F_{11})_2$ (cf. Figures 5 and 6), aggregation of the ligands to multinuclear entities shifts the F_2 elimination reactions to the Hg^{II} side and is thus actually unfavorable for the stability of the Hg^{IV} complexes. However, the additional exothermicity is only about -20 and about $-30\,kJ\,mol^{-1}$ for $Hg(As_2F_{11})_4$ and $HgF_2(As_2F_{11})_2$, respectively (Tables 3 and 4). In contrast, fluorine elimination from $HgF_2(Sb_2F_{11})_2$ is about 60 $kJ\,mol^{-1}$ more exothermic than from $HgF_2(SbF_6)_2$ (Tables 3 and 4), consistent with the above discussion of more pronounced differential aggregation effects for the antimony species. Once we consider also aggregation of formed SbF_5 (see above), the Hg^{IV} complexes with Sb_2F_{11} ligands exhibit rather unfavorable thermochemistry. In contrast, the As_2F_{11} complexes are only marginally less favorable than their respective AsF_6 analogues, and not much further energy penalty from aggregation of AsF_5 must be paid.

$X^- = OEF_5^-$ (E = Se, Te): Of the systems studied in this work, the complexes $HgF_2(OEF_5)_2$ (E = Se, Te) are the only ones that are thermochemically stable towards elimination of F_2. The reaction energies (Table 5) are about $+15$–$20\,kJ\,mol^{-1}$, not far below the $+44\,kJ\,mol^{-1}$ computed previously at the same theoretical level for the gas-phase reaction $HgF_4 \rightarrow HgF_2 + F_2$[10] (cf. Table 1). This is consistent with the similar *trans* influence of OEF_5 and fluorine ligands.[31]

However, the OEF_5 complexes have another pathway of elimination, namely, $HgF_2(OEF_5)_2 \rightarrow HgF_2 + (OEF_5)_2$ and $Hg(OEF_5)_4 \rightarrow Hg(OEF_5)_2 + (OEF_5)_2$, respectively (see above). Reaction energies for the former reaction range from about -100 to about $-110\,kJ\,mol^{-1}$ (without aggregation of HgF_2), and those for the latter reaction are between about -120 and about $-130\,kJ\,mol^{-1}$. One might expect,[31] that this is due to the relatively strong O–O bonds in the peroxides F_5EOOEF_5 compared to the weaker F–F bond in F_2.[39,40] However, the peroxide O–O bonds are only about 15–20 $kJ\,mol^{-1}$ more stable than the F–F bond (Table 5). This is clearly not enough to explain the much more facile elimination of X_2 compared to F_2. Notably, the O–O bonds in the substituted peroxides $(OEF_5)_2$ are actually 30–40 $kJ\,mol^{-1}$ weaker than in parent H_2O_2 (Table 5), in spite of the smaller bond length[41] (the bond is slightly stronger with E = Te than with E = Se). Thus, significantly weaker Hg–O than Hg–F bonds in the Hg^{IV} complexes must be the main reason for the more facile elimination of $(OEF_5)_2$ compared to fluorine. This is confirmed by fragmentation energies in Table 5: breaking of the two Hg–$OTeF_5$ bonds costs only about 60 $kJ\,mol^{-1}$ (40 $kJ\,mol^{-1}$ for Hg–$OSeF_5$), compared to about 190 $kJ\,mol^{-1}$ for two Hg–F bonds in HgF_4 (cf.

Table 1). Similar values apply to Hg–F and Hg–OEF_5 bonds in mixed complexes (Table 5). The overall fragmentation energies $HgX_4 \rightarrow Hg + 4X$ are more than 200 kJ mol^{-1} lower for $X = OEF_5$ than for X = F (Tables 1 and 5; but they are even larger than for X = Cl, at least in the case of teflate).

An expected advantage of the OEF_5 ligands is the volatility of their Hg^{II} complexes. To estimate the tendency towards aggregation, we computed the dimers of $Hg(OTeF_5)_4$ and $Hg(OTeF_5)_2$ (see Table S1 in Supporting Information for optimized coordinates). Both feature relatively weak intermolecular interactions and small distortions within the monomeric units. Dimerization energies are about −18.4 and about −47.0 kJ mol^{-1} for the Hg^{IV} and Hg^{II} systems, respectively (without CP corrections). This should be compared to dimerization energies of about −33.3 and about −60.7 kJ mol^{-1} computed for HgF_4 and HgF_2, respectively, at the same computational level (see refs. [1,42] for ab initio results). This suggests appreciably lower energies of aggregation. In particular, $Hg(OTeF_5)_2$ is not expected to aggregate to large units,[15,31] whereas HgF_2 forms an ionic fluorite-type lattice. We note in passing that dispersion effects are expected to be of minor importance for the aggregation of these particular fluorine-based systems,[42] and thus the DFT methods employed should provide reasonable estimates of the dimerization energies.

Bonding analyses: The role of relativistic effects in stabilizing $Hg^{IV}F_4$ against reductive elimination was found to arise mainly from a relativistic destabilization of $Hg^{II}F_2$, due to the relativistic contraction of the mercury 6s orbital.[1] The corresponding loss of ionic bonding contributions on the Hg^{II} side and the resulting relative stabilization of Hg^{IV} thus depend on the presence of very electronegative ligands like fluorine. This explains partly why $HgCl_4$ and HgH_4 are predicted to be strongly endothermic compounds.[9,10,11] Electronegativity considerations were thus important for the choice of weakly coordinating anions as ligands in the present work.

Table 6 shows that the EF_6 ligands provide appreciably larger positive metal charge in the Hg^{II} complexes, but only slightly more for the Hg^{IV} systems. This may partly be due to the tridentate bonding mode in the $Hg(EF_6)_2$ complexes (see Figure 4), but even in the Hg^{IV} complexes the EF_6 ligands can be considered more electronegative than fluorine. From this point of view, they are a reasonable choice in the present context. We think that the less favorable thermochemistry compared to (gas-phase) HgF_4 is mainly due to the coordination number of six in the Hg^{II} complexes. Individual atomic charges within the ligands (Table S3 in Supporting Information) provide further interesting insights into the bonding. For example, they show a much larger ionicity of Sb–F compared to As–F bonds. This is responsible for the more pronounced tendency of the antimony systems to aggregate (see above).

Table 6. Computed NPA fragment charges for EF_6 complexes (E = As, Sb).

	Hg	F	EF_6
HgF_2	1.460	−0.730	
HgF_4	2.113	−0.528	
$Hg(AsF_6)_2$	1.721		−0.860
$Hg(SbF_6)_2$	1.729		−0.865
trans-$HgF_2(AsF_6)_2$	2.162	−0.492	−0.589
cis-$HgF_2(AsF_6)_2$	2.161	−0.470	−0.611
trans-$HgF_2(SbF_6)_2$	2.190	−0.465	−0.630
cis-$HgF_2(SbF_6)_2$	2.180	−0.436	−0.654
$Hg(AsF_6)_4$	2.164	−0.485[a]	−0.597[a]
$Hg(SbF_6)_4$	2.204		−0.551

[a] Only two intact AsF_6 ligands, see Figure 3a.

There has been appreciable discussion whether the OEF_5 ligands (E = Se, Te) exhibit higher or lower electronegativity than fluorine. Different experimental measures gave rise to opposite conclusions.[31] The charges for the mercury complexes in Table 7 show a mixed situation: metal charges of the $Hg^{II}(OEF_5)_2$ complexes are somewhat more positive than in HgF_2. This would suggest slightly larger electronegativity. The situation is reversed for the Hg^{IV} complexes, with slightly lower negative charges for OEF_5 compared to F. This confirms the "soft" nature of the electronegativity concept. In any case, the NPA charges confirm the similarity of the electronegativities of OEF_5 and F.

Table 7. Computed NPA fragment charges for OEF_5 complexes (E = Se, Te).

	Hg	F	OEF_5
HgF_2	1.460	−0.730	
HgF_4	2.113	−0.528	
$Hg(OSeF_5)_2$	1.519		−0.760
$Hg(OTeF_5)_2$	1.521		−0.760
trans-$HgF_2(OSeF_5)_2$	2.051	−0.533	−0.492
cis-$HgF_2(OSeF_5)_2$	2.053	−0.528	−0.499
trans-$HgF_2(OTeF_5)_2$	2.059	−0.529	−0.500
cis-$HgF_2(OTeF_5)_2$	2.061	−0.527	−0.503
$Hg(OSeF_5)_4$	1.970		−0.493
$Hg(OTeF_5)_4$	1.979		−0.495

Why are the Hg–OEF_5 bonds much weaker than the Hg–F bonds in the Hg^{IV} species (see Table 5)? Local charge differences around the donating atoms (Table S3c,d in Supporting Information) provide an explanation: Owing to the bonding of the oxygen atom in the OEF_5 complexes to two relatively electropositive centers (Hg and E), it aquires much higher negative charge (ca. −1.0) than the fluorine atoms (ca. −0.5) in HgF_4 or HgF_2X_2. This leads to appreciably larger antibonding interactions with the formally nonbonding d electrons in the $5d^8$ complex. This can be seen, for example, from inspection of the highest occupied MOs of the $HgF_2(OTeF_5)_2$ systems (not shown), which exhibit much more pronounced Hg–O than Hg–F antibonding interactions. In consequence, the Hg–O bonds are weakened relative to Hg–F bonds due to the relatively high negative local charge on oxygen.

Discussion and Suggestions for Experimental Investigation

None of the Hg^{IV} complexes investigated here is thermochemically stable, as they all exhibit one exothermic pathway for reductive elimination. In the case of AlF_4, Al_2F_7, EF_6, and E_2F_{11} ligands (E = As, Sb), elimination of F_2 is exothermic with reaction energies varying between −60 and −180 kJ mol^{-1}. In this sense, the systems are clearly inferior to gas-phase HgF_4, which eliminates F_2 endothermically.[1,6,9,10] However, based on previous estimates and the relatively high sublimation energy of HgF_2,[1] we think that several of these complexes may provide a more favorable environment for Hg^{IV} than HgF_4 itself in the condensed phase. Indeed, the relatively high sixfold coordination of many of the HgX_2 elimination products (Figures 2, 4, and 6) indicates that even these weakly coordinating anions are able to stabilize the more ionic Hg^{II} better than the more covalent Hg^{IV}. The situation is thus indeed intermediate between those of gas- and condensed-phase HgF_4. We note also that the more stable of the systems studied here are predicted to be less endothermic than (gas-phase) $HgCl_4$ or HgH_4 (see Table 1).[9–11]

Are the systems investigated here promising targets for experimental study? In view of the computed endothermicity of all complexes with respect to F_2 or X_2 elimination, the answer to this question depends on the presence of sufficiently high activation barriers for the reductive elimination reactions. Unfortunately, the complicated electronic structure of the transition state does not allow us at this point to provide these activation barriers quantitatively. The transition state for H_2 elimination from HgH_4 in the gas phase is comparably easy to locate.[10,11] It exhibits C_{2v} symmetry and is about 50 kJ mol^{-1} above HgH_4 (about 250 kJ mol^{-1} above $HgH_2 + H_2$). Unfortunately, we found that the barriers for F_2 elimination from HgF_4 and for Cl_2 elimination from $HgCl_4$ are much more difficult to compute, due to large nondynamic correlation effects.[10] These seem to be related to repulsions between lone-pair electrons on the halide ligands and the semicore 5p shell on the metal atom. The transition state has in both cases appreciable multireference character and is not described correctly by single-reference coupled-cluster approaches or by DFT methods. As the active space for a multiconfiguration self-consistent field (CASSCF) wavefunction must include the metal d orbitals and several orbitals from the ligands, the required expansions for a multireference configuration interaction (MRCI) calculation are expected to be large. We currently perform such calculations for HgF_4 itself. However, there is no realistic chance to obtain reliable activation barriers for the larger systems studied here with currently available computational resources. The DFT and CCSD(T) calculations, although certainly unreliable quantitatively, provided considerably larger barriers for X_2 elimination from HgX_4 (X = F, Cl) than for X = H.[10] Intuitively, this appears reasonable, as the electronic reorganization on splitting two Hg−X bonds with formation of the X−X bond and rearrangement of the HgX_2 framework is expected to be much more pronounced for the halide complexes than for their hydride analogue. This should hold largely also for the related larger HgX_4 and HgF_2X_2 systems studied here. It is therefore quite likely that most of the Hg^{IV} systems investigated in this work will have appreciable barriers for F_2 and X_2 elimination. As the exothermicity of most elimination reactions computed is much more moderate than, for example, that of $HgH_4 \rightarrow HgH_2 + H_2$ (see Tables 1–5), the chances of observing some of the computed Hg^{IV} minima appear quite realistic.

Thermochemically, the AsF_6 and As_2F_{11} complexes are already more favorable than their SbF_6 and Sb_2F_{11} analogues when we consider only small molecular complexes as products. The computed thermochemistry of Hg^{IV} complexes with SbF_6 or Sb_2F_{11} ligands turned out to be somewhat disappointing. This became even clearer when the much more pronounced aggregation of SbF_5 compared to AsF_5 was taken into account. The exothermicity of F_2 elimination from $Hg(AsF_6)_4$ or from $HgF_2(AsF_6)_2$ may be considered very moderate indeed. Moreover, we also do not expect much further stabilization of the elimination products $Hg^{II}X_2$ ($X^- = AsF_6^-$, $As_2F_{11}^-$) by aggregation. This may indeed leave appreciable room for finding suitable reaction conditions. The obvious practical disadvantage of an AsF_5 (m.p. −79.8 °C, b.p. −52.8 °C) compared to an SbF_5 (m.p. 8.3 °C, b.p. 141 °C) matrix environment is the need to work at low temperatures. On the other hand, in view of the endothermicity of the target complexes, and in the absence of reliable reaction barriers, low-temperature reaction conditions are in any case recommended. The high volatility of AsF_5 might prove favorable for product isolation. Possible oxidizing agents are elemental fluorine (possibly with irradiation to create fluorine atoms) or, for example, KrF_2.

Complexes with the OEF_5 anions (E = Se, Te) are distinguished by their preference to bind primarily in a monodentate fashion through their single oxygen atom, even for the Hg^{II} elimination products (see Figure 8). Weak additional secondary bonding is present but appears both for the Hg^{II} and Hg^{IV} systems. Consequently, the complexes $HgF_2(OEF_5)_2$ are the only systems studied here that exhibit endothermic elimination of F_2 with energetics that are almost competitive with those of gas-phase HgF_4 (see Table 5). Notably, aggregation of the Hg^{II} complexes is expected to provide only relatively little further stabilization relative to Hg^{IV} in these systems (cf. dimerization energies above). This agrees with the fact that the well-known $Hg(OEF_5)_2$ complexes are essentially molecular. In contrast to HgF_2 (but more like $HgCl_2$), they are volatile and have a high vapor pressure even at room temperature. They thus sublime easily and they dissolve molecularly in nonpolar solvents.[15,31] Notably, the secondary Hg···F contacts in the optimized structures appear to be comparable for the Hg^{IV} and Hg^{II} species (see Figures 7 and 8, respectively). We have thus come very close to our goal of an almost gas-phase-like environment in the condensed phase.

Unfortunately, the complexes of OEF_5 ligands are not unchallenged champions either, as they eliminate $(OEF_5)_2$ exothermically, with energies that are similar to those of F_2 elimination from some of the other systems studied here. As shown above, this is only in small part due to the stronger O–O than F–F bond. It reflects mainly the destabilization of the Hg–O bonds in the Hg^{IV} complexes by larger antibonding interactions. Another reaction pathway known for teflate complexes of transition metals in high oxidation states is elimination of TeF_6 and $F_5TeOTeF_5$ (e.g., to give $O{=}Re(OTeF_5)_5$ from $Re(OTeF_5)_7$).[31] This is very unlikely to occur in the present case, as steric crowding is not a problem for the Hg^{IV} complexes (anyway, the reaction would retain Hg^{IV}).

In any case, the $Hg(OTeF_5)_4$ and $HgF_2(OTeF_5)_2$ complexes appear to be interesting targets for synthetic work. How could they be prepared? The Hg^{II} complexes $Hg(OEF_5)_2$ (E = Se, Te) are well known.[31,40] They might be a good starting point. A variety of suitable reagents for oxidations are available, including $Xe(OTeF_5)_2$,[31,40] $Xe(OTeF_5)_4$,[34] or the recently reported $[XeOTeF_5][Sb(OTeF_5)_6]$.[43] $B(OTeF_5)_3$ is also a well-known reagent for transferring the $OTeF_5$ ligand.[31] It could be supplemented by a suitable oxidizing agent. Moreover, the backreaction of exothermic X_2 elimination in Table 5 appears attractive: photolytic cleavage of the peroxidic bond in $(OTeF_5)_2$ would create the reactive $^{\bullet}OTeF_5$ radical, which should add exothermically to $Hg(OTeF_5)_2$ (cf. Table 5). The Hg^{IV} complexes could be characterized by IR spectroscopy (see computed vibrational frequencies in Table S2 in the Supporting Information) or by NMR spectroscopy for various nuclei (^{19}F, ^{17}O, ^{199}Hg, ^{125}Te; we currently compute NMR parameters for many complexes).[31]

Comparison with noble-gas teflate complexes provides further support for our optimistic view on the possible preparation of Hg^{IV} teflate systems: $Xe(OTeF_5)_2$ exhibits surprisingly high thermal stability and decomposes only above about 130 °C ($Xe(OSeF_5)_2$ is only slightly less stable).[31,40] Nevertheless, our computations show that $Xe(OTeF_5)_2$ is endothermic with respect to elimination of $(OTeF_5)_2$, with a reaction energy in a similar range as computed for the Hg^{IV} complexes (Table 8). Similarly, $Xe(OTeF_5)_4$ is well known but computed to eliminate $(OTeF_5)_2$ with even slightly higher exothermicity than $Hg(OTeF_5)_4$ (cf. Tables 5 and 8). There is even some NMR evidence for the formation of $Kr(OTeF_5)_2$, the first compound with a Kr–O bond, in cocondensation reactions between KrF_2 and $B(OTeF_5)_3$, although the compound could not be isolated in pure form.[44] According to our computations, $Kr(OTeF_5)_2$ is more endothermic than any of our Hg^{IV} teflate candidates. In fact, our calculations even give a slightly negative energy for fragmentation into $Kr + 2\,^{\bullet}OTeF_5$ (Table 8). For this rather unstable system, the DFT results are probably too low (our validation did not include such noble gas systems). The MP2 calculations provide more positive fragmentation energies, which in turn are probably far too high (MP2 and B3LYP agree much better with each other and with available experimental data for more stable noble gas/fluoride systems; see Table 8). In any case, the thermochemical viability of many of the Hg^{IV} complexes studied here appears superior to that of $Xe(OTeF_5)_4$ or $Kr(OTeF_5)_2$. As in the Hg^{IV} case (see above), elimination of $(OTeF_5)_2$ from the noble gas (NG) teflate complexes is much more facile than that of F_2 from the fluorides (Table 8), which reflects appreciably weaker NG–$OTeF_5$ than NG–F bonds. We finally quote the well-known KrF_2 (Table 8), which exhibits an endothermicity that is not much lower than that discussed for several of our more promising target systems.

Table 8. Reaction energies [kJ mol^{-1}] for noble gas complexes.

Reaction	ΔE_{calcd}[a]	ΔH_{exptl}[b]
$Xe(OTeF_5)_4 \rightarrow Xe(OTeF_5)_2 + (OTeF_5)_2$ (D_{2d})[c]	−139.2	
$Xe(OTeF_5)_4 \rightarrow Xe(OTeF_5)_2 + (OTeF_5)_2$ (C_{2h})[d]	−149.0	
$Xe(TeOF_5)_2 \rightarrow Xe + (OTeF_5)_2$	−80.7 (−66.4)	
$Kr(TeOF_5)_2 \rightarrow Kr + (OTeF_5)_2$	−194.3 (−96.5)	
$Xe(TeOF_5)_2 \rightarrow Xe + 2\,^{\bullet}OTeF_5$	+101.5 (+181.4)	
$Kr(TeOF_5)_2 \rightarrow Kr + 2\,^{\bullet}OTeF_5$	−12.2 (+151.3)	
$(OTeF_5)_2 \rightarrow 2\,^{\bullet}OTeF_5$	+182.2 (+247.8)	
$XeF_4 \rightarrow XeF_2 + F_2$	+72.5 (+86.5)	+119.5
$XeF_2 \rightarrow Xe + F_2$	+93.6 (+86.7)	+117.9
$KrF_2 \rightarrow Kr + F_2$	−46.6 (−65.7)	−60.2
$XeF_2 \rightarrow Xe + 2\,^{\bullet}F$	+247.8	+267.5
$KrF_2 \rightarrow Kr + 2\,^{\bullet}F$	+107.5	+97.8

[a] B3LYP results with MP2 values in parentheses. [b] See N. Bartlett, F. O. Sladky in *Comprehensive Inorganic Chemistry*, *Vol. 1*, Pergamon, Oxford, **1973**, Chap 6. Note that the reported experimental energies are not completely consistent with the binding energy of F_2 (cf. footnote b to Table 5). [c] More stable alternating structure of $Xe(OTeF_5)_4$. [d] Less stable nonalternating arrangement of $Xe(OTeF_5)_4$ as found in the solid-state structure.[34]

Conclusion

The quest for Hg^{IV} continues. Promising avenues exist which have not yet been pursued experimentally. On the one hand, the matrix-isolation route to HgF_4 deserves more attention than it has received hitherto. On the other hand, the present work provides a quantum-chemical study of species that might be obtainable in the bulk condensed phase and could thus open a true Hg^{IV} chemistry. While all Hg^{IV} complexes discussed here exhibit one pathway of exothermic reductive elimination, we have reason to believe that many systems will have nonnegligible activation barriers along the way and might thus be observable, at least at low temperatures. This holds in particular for complexes like $Hg(OTeF_5)_4$ or $Hg(AsF_6)_4$. We have furthermore suggested a number of possible synthetic routes towards such systems. However, we are convinced that the ingenuity of our experimental colleagues will come up with further options that we were not able to envision. The chances to finally enter experimentally into Hg^{IV} chemistry are therefore good, and we hope that the present computational study will provide additional motivation for further experimental research.

Acknowledgement

We are grateful to Dr. Roman Reviakine for technical assistance. This work has been supported by Deutsche Forschungsgemeinschaft (M.K.) and by Emil Aaltonen foundation (M.S.). Computational resources were partially provided by the Center of Scientific Computing, Espoo, Finland.

---

[1] M. Kaupp, M. Dolg, H. Stoll, H. G. von Schnering, *Inorg. Chem.* **1994**, *33*, 2122.
[2] M. Seth, P. Schwerdtfeger, M. Dolg, *J. Chem. Phys.* **1997**, *106*, 3623.
[3] R. L. Deming, A. L. Allred, A. R. Dahl, A. W. Herlinger, M. O. Kestner, *J. Am. Chem. Soc.* **1976**, *98*, 4132.
[4] Indeed, the EPR data reported[3] for $[Hg^{III}(cyclam)]^{3+}$ do not look much like one would expect for a $5d^9$ complex.
[5] C. K. Jørgensen, *J. Chem. Phys.* **1979**, *76*, 630. C. K. Jørgensen, *Z. Anorg. Allg. Chem.* **1986**, *540/541*, 91.
[6] M. Kaupp, H. G. von Schnering, *Angew. Chem.* **1993**, *105*, 952; *Angew. Chem. Int. Ed. Engl.* **1993**, *32*, 861.
[7] P. Schwerdtfeger, P. D. W. Boyd, S. Brienne, J. McFeaters, M. Dolg, M.-S. Liao, W. H. E. Schwarz, *Inorg. Chim. Acta* **1993**, *213*, 233.
[8] P. Schwerdtfeger, P. D. W. Boyd, S. Brienne, A. K. Burrell, *Inorg. Chem.* **1991**, *30*, 3481; P. Schwerdtfeger, *J. Am. Chem. Soc.* **1989**, *111*, 7261; P. Schwerdtfeger, M. Dolg, W. H. E. Schwarz, G. A. Bowmaker, P. D. W. Boyd, *J. Chem. Phys.* **1989**, *91*, 1762.
[9] W. Liu, R. Franke, M. Dolg, *Chem. Phys. Lett.* **1999**, *302*, 231.
[10] S. Riedel, M. Straka, M. Kaupp, *Phys. Chem. Chem. Phys.* **2004**, *6*, 1122.
[11] P. Pyykkö, M. Straka, M. Patzschke, *Chem. Commun.* **2002**, 1728.
[12] K. Millington, PhD Thesis, University of Southhampton, United Kingdom, **1987** (I. R. Beattie, personal communication to M.K., **1993**). See also I. R. Beattie, *Angew. Chem.* **1999**, *111*, 3494; *Angew. Chem. Int. Ed.* **1999**, *38*, 3294.
[13] S. Riedel, M. Straka, M. Kaupp, unpublished results.
[14] I. Krossing, I. Raabe, *Angew. Chem.* **2004**, *116*, 2116; *Angew. Chem. Int. Ed.* **2004**, *43*, 2066.
[15] S. H. Strauss, *Chem. Rev.* **1993**, *93*, 927.
[16] A. D. Becke, *J. Chem. Phys.* **1993**, *98*, 5648.
[17] C. Lee, W. Yang, R. G. Parr, *Phys. Rev. B* **1988**, *37*, 785. B. Miehlich, A. Savin, H. Stoll, H. Preuss, *Chem. Phys. Lett.* **1989**, *157*, 200.
[18] Gaussian 98, Revision A.1, M. J. Frisch, G. W. Trucks, H. B. Schlegel, G. E. Scuseria, M. A. Robb, J. R. Cheeseman, J. A. Montgomery, J. T. Vreven, K. N. Kudin, J. C. Burant, J. M. Millam, S. S. Iyengar, J. Tomasi, V. Barone, B. Mennucci, M. Cossi, G. Scalmani, N. Rega, G. A. Petersson, H. Nakatsuji, M. Hada, M. Ehara, K. Toyota, R. Fukuda, J. Hasegawa, M. Ishida, T. Nakajima, Y. Honda, O. Kitao, H. Nakai, M. Klene, X. Li, J. E. Knox, H. P. Hratchian, J. B. Cross, C. Adamo, J. Jaramillo, R. Gomperts, R. E. Stratmann, O. Yazyev, A. J. Austin, R. Cammi, C. Pomelli, J. W. Ochterski, P. Y. Ayala, K. Morokuma, G. A. Voth, P. Salvador, J. J. Dannenberg, V. G. Zakrzewski, S. Dapprich, A. D. Daniels, M. C. Strain, O. Farkas, D. K. Malick, A. D. Rabuck, K. Raghavachari, J. B. Foresman, J. V. Ortiz, Q. Cui, A. G. Baboul, S. Clifford, J. Cioslowski, B. B. Stefanov, G. Liu, A. Liashenko, P. Piskorz, I. Komaromi, R. L. Martin, D. J. Fox, T. Keith, M. A. Al-Laham, C. Y. Peng, A. Nanayakkara, M. Challacombe, P. M. W. Gill, B. Johnson, W. Chen, M. W. Wong, C. Gonzalez, J. A. Pople, Gaussian, Inc., Pittsburgh PA, **2003**.
[19] R. Ahlrichs, M. Bär, M. Häser, H. Horn, C. Kölmel, *Chem. Phys. Lett.* **1989**, *162*, 165; R. Ahlrichs, M. von Arnim in *Methods and Techniques in Computational Chemistry: METECC95* (Eds.: E. Clementi, G. Corongiu), STEF, Cagliari, **1995**, pp. 509 ff.
[20] M. Seth, F. Cooke, P. Schwerdtfeger, J.-L. Heully, M. Pellisier, *J. Chem. Phys.* **1998**, *109*, 3935.
[21] U. Haeussermann, M. Dolg, H. Stoll, H. Preuss, P. Schwerdtfeger, R. M. Pitzer, *Mol. Phys.* **1993**, *78*, 1211.
[22] A. Bergner, M. Dolg, W. Kuechle, H. Stoll, H. Preuss, *Mol. Phys.* **1993**, *80*, 1431.
[23] M. M. Francl, W. J. Pietro, W. J. Hehre, J. S. Binkley, M. S. Gordon, D. J. DeFrees, J. A. Pople, *J. Chem. Phys.* **1982**, *77*, 3654.
[24] S. Huzinaga, J. Anzelm, M. Klobukowski, E. Radzio-Andzelm, Y. Sakai, H. Tatewaki, *Gaussian Basis Sets for Molecular Calculations*, Elsevier, Amsterdam, **1984**.
[25] A. Nicklaß, M. Dolg, H. Stoll, H. Preuss, *J. Chem. Phys.* **1995**, *102*, 8942.
[26] T. Clark, J. Chandrasekhar, G. W. Spitznagel, P. von R. Schleyer, *J. Comput. Chem.* **1983**, *4*, 294.
[27] A. E. Reed, F. Weinhold, *J. Chem. Phys.* **1985**, *83*, 1736.
[28] NBO4.M version of NBO analysis programs, by F. Weinhold et al., University of Wisconsin, **1999**.
[29] R. Reviakine, unpublished results, Würzburg **2004**.
[30] See for example A. F. Holleman, E. Wiberg, *Lehrbuch der Anorganischen Chemie*, 71–101th ed., Walter de Gruyter, Berlin, **1995**. N. N. Greenwood, A. Earnshaw, *Chemistry of the Elements*, Pergamon Press, Oxford, **1984**.
[31] K. Seppelt, *Angew. Chem.* **1982**, *94*, 890; *Angew. Chem. Int. Ed. Engl.* **1982**, *21*, 877.
[32] S. Raugei, M. L. Klein, *J. Chem. Phys.* **2002**, *116*, 7087. D. Kim, M. L. Klein, *J. Phys. Chem. B* **2000**, *104*, 10074. See also: P. M. Estevez, A. Ramirez-Solis, C. J. A. Mota, *J. Am. Chem. Soc.* **2002**, *124*, 2672.
[33] P. Huppmann, H. Hartl, K. Seppelt, *Z. Anorg. Allg. Chem.* **1985**, *524*, 26.
[34] L. Turovsky, K. Seppelt, *Z. Anorg. Allg. Chem.* **1992**, *609*, 153.
[35] P. K. Miller, K. D. Abney, A. K. Rappé, O. P. Anderson, S. H. Strauss, *Inorg. Chem.* **1988**, *27*, 2255.
[36] P. Zylka, H. Oberhammer, K. Seppelt, *J. Mol. Struct.* **1991**, *243*, 411.
[37] *CRC Handbook of Chemistry and Physics*, 68th Ed, (Ed. R. C. Weast), CRC Press, Boca Raton, **1987–1988**.
[38] See for example R. Minkwitz, F. Neikes, *Inorg. Chem.* **1999**, *38*, 5960; K. O. Christe, X. Zhang, R. Bau, J. Hegge, G. A. Olah, G. K. S. Prakash, J. A. Sheehy, *J. Am. Chem. Soc.* **2000**, *122*, 481, and references therein.
[39] K. Seppelt, *Z. Anorg. Allg. Chem.* **1973**, *399*, 87; H. A. Carter, J. N. M. Shreeve, *Spectrochim. Acta* **1973**, *29*, 1321.
[40] K. Seppelt, D. Nothe, *Inorg. Chem.* **1973**, *12*, 2727.
[41] This lack of correlation between bond lengths and binding energies is not uncommon in the case of substitution by electronegative groups. It can be traced back to an interplay between electrostatic contraction effects and hybridization defects (cf. M. Kaupp, B. Metz, H. Stoll, *Angew. Chem.* **2000**, *112*, 4780; *Angew. Chem. Int. Ed. Angew. Chem. Int. Ed. Engl.* **2000**, *39*, 4607; M. Kaupp, S. Riedel, *Inorg. Chim. Acta* **2004**, *357*, 1865, and references therein).
[42] M. Kaupp, H. G. von Schnering, *Inorg. Chem.* **1994**, *33*, 2555, 4718.
[43] H. P. A. Mercier, M. D. Moran, G. J. Schrobilgen, C. Steinberg, R. J. Suontamo, *J. Am. Chem. Soc.* **2004**, *126*, 5533.
[44] J. C. P. Sanders, G. J. Schrobilgen, *J. Chem. Soc. Chem. Commun.* **1989**, 1576.

Received: November 8, 2004